LITERATURE CITED

Carmichael, L. T., and B. H. Sage, "Thermal Conductivity of Fluids, n-Butane," *J. Chem. Eng. Data*, **9**, 511 (1964).

Gilmore, T. F., and E. W. Comings, "Thermal Conductivity of Binary Mixtures of Carbon Dioxide, Nitrogen, and Ethane at High Pressures: Comparison with Correlation and Theory," *AIChE J.*, **12**, 1172 (1966).

Goodwin, R. D., "The Thermophysical Properties of Methane from 90 to 500 K at Pressures to 700 Bar," NBS Technical Note No. 653, Washington, DC (1974).

Hanley, H. J. M., R. D. McCarty, and W. M. Haynes, "Equations for the Viscosity and Thermal Conductivity Coefficients of Methane," *Cryogenics*, **15**, 413 (1975).

Leach, J. W., P. S. Chappelear, and T. W. Leland, "Properties of Hydrocarbon and Quantum Gas Mixtures from the Corresponding States Principle," *Proc., Amer. Petrol. Inst.*, **46**, 223 (1966).

Murad, S., and K. E. Gubbins, "Corresponding States Correlation for Thermal Conductivity of Dense Fluids," *Chem. Eng. Sci.*, **32**, 499 (1977).

Manuscript received June 25, 1980; revision received October 7, and accepted October 21, 1980.

Deviations of Actual Minimum Fluidization Velocities from Theoretical Predictions at Different Temperatures

KAREL SVOBODA

and

MILOSLAV HARTMAN

Institute of Chemical Process Fundamentals
Czechoslovak Academy of Sciences
Prague, Czechoslovakia

The incipient fluidization velocity is one of the fundamental parameters in modeling fluidized bed processes. Although most fluidized bed applied in industry operate well above room temperature, there is, in general, little known about fluidization at elevated or high temperatures. Only few studies reporting data on the variation of onset of fluidization with temperature can be found in the literature.

With temperature increase the density and viscosity of a gas change in a definite, well known way. In dependence on the type of material, the particle diameter and density are also affected by temperature. Unfortunately, accurate data on the thermal expansion at high temperatures can be found in the literature only for very few materials. Some calculations showed that this effect should be small. It is assumed in the present work that the effect of temperature on the particle diameter and density is negligible. Recent works of Desai et al. (1977) and Doheim and Collinge (1978) suggest a possible influence of temperature on properties of the solid particle bed.

Effort to separate the effect of temperature on the properties of gas from those of particle bed led to a simple linear equation (Desai et al., 1977):

$$\log G_{mf} = -a \log T + b \tag{1}$$

Originally, this equation was developed for laminar gas flow region, where viscous effect predominate, i.e., approximately for $Re_{mf} < 2$.

A practical meaning of Eq. 1 is apparent. When the coefficient a is known, the minimum fluidization velocity at temperature of interest can be predicted from a single measurement at room temperature.

Theoretically, the coefficient a in Eq. 1 depends only on the properties of fluidizing medium, i.e., $a = a(\mu_g, \rho_g)$. Its value shows how the incipient velocity changes when temperature varies. The other coefficient $b = b(d_p, \epsilon, \psi,$ gas species) combines effects of material constants, particle bed characteristics and gas properties as well.

The values of the coefficient $(a)_{exp}$ reflect actual overall changes in the minimum fluidization velocities U_{mf} with temperature found by experiments. This offers a rational basis for verification of the theoretical predictions.

The gas density is inversely proportional to the absolute temperature and the viscosity of air is given with accuracy better than 3% by the relation:

$$\mu_g = 1.81 \times 10^{-5}\left[\frac{T}{293}\right]^{0.66} \tag{2}$$

It follows from this that the theoretical value of a for air is about 1.66 in the laminar flow region ($Re_{mf} < 2$). For turbulent flow ($Re_{mf} > 1000$), where inertia effects predominate, the expected value of a is 0.5. In the transition flow region ($2 < Re_{mf} < 1000$) the coefficient a should decrease with increasing Reynolds numbers. With respect to the illustrative form of Eq. 1, it is convenient to evaluate the effect of temperature on G_{mf} also in the transition or turbulent region with the aid of this relation.

The purpose of the present work is to find by experiments in a wide temperature range the coefficients a and b in Eq. 1 for various materials and different particle sizes. The experimental values are compared with values $(a)_{calc}$ and $(b)_{calc}$ predicted from different equations for U_{mf} summarized in Table 1.

EXPERIMENTAL

Materials. The minimum fluidization velocity was determined from pressure drop—gas velocity data measured at different temperatures. Bed materials were chosen with respect to their occurrence in a fluidized bed for combustion of brown coal and simultaneous SO_2 removal. The particle and bed properties of limestone, lime, brown coal ash and corundum used in the work are presented in Table 2. The last material was chosen as a comparing standard for its well defined physical properties. The particles of coal ash were almost flake-like, the particles of limestone and lime were of irregular shapes, nevertheless, they appeared quite isometrical when examined by a microscope. The particles of sintered corundum were ellipsoidal ones with a smooth surface.

Apparatus. Measurements of U_{mf} were performed in a 0.085 m I.D. steel, electrically heated reactor the height of which was $H_K = 0.5$ m. The fluidizing air was well preheated to a desired temperature prior to being introduced through a plate distributor into the bed of particles. Temperature in the bed was measured by the thermocouple Pt—Rh10 Pt. The pressure drop across the bed was measured by means of a pressure probe and U-tube manometer.

Procedure. The particle bed of height $H = D_K$ was heated to a desired temperature and the flow rate of air was gradually reduced from a well fluidized state to a static bed. The pressure drops and corresponding air flow rates were recorded and the minimum fluidization velocity was then determined from the plot pressure drop vs. velocity of air. The measurements of U_{mf} were carried out on eight levels of temperature in the range 20-890°C. In the case of limestone temperatures up to 450°C

0001-1541-81-4815-0866-$2.00.

TABLE 1. EQUATIONS EMPLOYED TO PREDICT THE MINIMUM FLUIDIZATION VELOCITY

Equation	No. of equation	Author
$Ga = \frac{150(1-\epsilon_{mf})}{\epsilon_{mf}^3 \cdot \psi^2} Re_{mf} + \frac{1.75}{\epsilon_{mf}^3 \cdot \psi} Re_{mf}^2$	(3)	Ergun (1952)
$\epsilon_{mf}^{4.7}\, \psi^2\, Ga = 18\, Re_{mf} + 2.7\, \psi^{0.687}\, Re_{mf}^{1.687}$	(4)	Wen and Yu (1966) cited in Saxena and Vogel (1977)
$\frac{g(\rho_s - \rho_g)\bar{d}_p}{\rho_g U_{mf}^2} = 2.42 \times 10^5 \left[\frac{\mu_g^2}{\rho_g(\rho_s-\rho_g)g\bar{d}_p^3}\right]^{0.85} \left[\frac{\rho_s}{\rho_g}\right]^{0.13} + 37.7$	(5)	Broadhurst and Becker (1975)
$Re_{mf} = \frac{Ga}{1400 + 5.22\sqrt{Ga}}$	(6)	Todes (1957) cited in Syromjatnikov and Volkov (1959)
$\frac{U_{mf}}{3\sqrt{g \cdot \nu_g}} = 0.025\, [\bar{d}_p \cdot 3\sqrt{g/\nu_g^2}]^{1.3} \left[\frac{\rho_s - \rho_g}{\rho_g}\right]^{0.6} \pi_c^{0.33}$ where $\pi_c = 1$ and $\bar{d}_p \cdot \sqrt[3]{g/\nu_g^2} \leq 3$	(7)	Sosna and Kondukov (1968)

were used. The overall experimental error in determination of U_{mf} varied with temperature and was less than 6-9%.

RESULTS AND DISCUSSION

In our experimental conditions the Reynolds numbers Re_{mf} varied from 0.3 to 36.8. The values $(G_{mf})_{exp}$ for $Re_{mf} < 20$ were used in evaluation of the parameters $(a)_{exp}$ and $(b)_{exp}$ in Eq. 1 by a least square method. Theoretical values of the coefficients $(a)_{calc}$ and $(b)_{calc}$ were determined by the same computational procedure using the values $(G_{mf})_{calc}$ predicted for different temperatures by individual equations summarized in Table 1. All these equations can be applied over a wide range of Re_{mf}.

The values of ϵ_{mf} needed in the computations were approximated by the values of ϵ_p obtained by repeated pouring the particles carefully from a container into the measuring cylinder. The particle sphericity ψ was evaluated from pressure drop measurements across fixed bed with the aid of the Ergun (Eq. 3).

The coefficients a and b determined from both experimental and computed dependences of G_{mf} on temperature are presented in Tables 3 and 4. The results obtained for the limestone particles are also shown in Figure 1.

At room temperature the onset of fluidization always occurred in the transition zone for $5.2 < Re_{mf} < 36.7$. At the highest temperatures of experiments fluidization often started in the laminar flow as $0.31 < Re_{mf} < 8.8$. The mean values of $\bar{Re}_{mf}$ were

TABLE 2. PHYSICAL PROPERTIES OF SOLIDS

Material	Size range (mm)	$\bar{d}_p$ (mm)	ρ_s (kg/m³)	ϵ_p (−)	ψ (−)	Range of $(Re_{mf})_{exp}$
Corundum	0.80-0.90	0.850	3330	0.430	0.819	1.89-25.6
Limestone	0.50-0.63	0.565	2220	0.460	0.780	1.36- 7.23
	0.63-0.80	0.715		0.456	0.801	2.66-13.5
	0.80-1.00	0.900		0.460	0.780	5.27-26.5
	1.00-1.25	1.125		0.462	0.724	8.77-36.8
Lime	0.50-0.63	0.565	1340	0.515	0.704	0.31- 5.17
	0.63-0.80	0.715		0.510	0.694	0.76- 9.85
	0.80-1.00	0.900		0.505	0.708	1.14-18.1
	1.00-1.25	1.125		0.501	0.670	2.22-27.2
Brown Coal Ash	0.50-0.63	0.565	1680	0.596	0.541	0.51- 8.27
	0.63-0.80	0.715		0.590	0.541	1.14-12.9
	0.80-1.00	0.900		0.600	0.520	1.85-19.4
	1.00-1.25	1.125		0.582	0.524	3.15-34.2

in all cases larger than two and thus the coefficients a presented in this work correspond to the transition zone close to laminar flow. The experimental values of a decrease with increasing Re_{mf} and, therefore, the particle diameter and lie in the interval $\langle 1.2, 1.59\rangle$. This finding is in accordance with theory by which $0.5 \leq a \leq 1.66$. While the coefficients a_{exp} for limestone and coal ash are practically the same the corresponding values for lime and corundum are somewhat higher. However, a limited number of data and their scatter do not allow to resolve clearly the question whether the coefficient a is effected by the properties of particles or not.

Desai et al. (1977) and Doheim and Collinge (1978) worked with particles as large as 0.1-0.2 mm but their coefficients a_{exp} varied from 1.25 to 1.35. These values are considerably lower than the trend of our experimental data suggests. This can probably be related to nonhomogenities of the bed caused by broad size distribution of the materials which the authors used. Our experimental data were obtained with narrow fractions of the particles under carefully controlled conditions and it seems to be the reason why our results are in a better agreement with theory.

The values of $(a)_{calc}$ predicted for different particle size by the individual equations listed in Table 1 follow well the trend of the experimental data except the equation of Sosna and Kondukov (1968). The least differences between $(a)_{exp}$ and $(a)_{calc}$ were found with theoretical predictions of Wen and Yu (1966) and those of Todes (1957). On the other hand, the results computed from the Ergun equation, on which most other correlations are based, show the largest deviations from the experimental values. For all materials and particle sizes tested the values of $(a)_{calc}$ are considerably higher than found by the experiments. In other words, it means that the equation of Ergun overestimates the effect of temperature on the onset of fluidization.

The fact that the influence of temperature on G_{mf} is less than predicted by the Ergun equation, can be explained by a possible increase of ϵ_{mf} with temperature or by variation of Ergun equation constants with increasing temperature.

The idea of change of ϵ_{mf} or structure of particle bed caused by temperature is supported by the results of Broadhurst and Becker (1975), who presented an empirical correlation for the voidage of a particle bed at the minimum bubbling point:

$$\epsilon_{mf} \doteq \epsilon_{mb} = \frac{0.586}{\psi^{0.72}} \left[\frac{\mu_g^2}{\rho_g(\rho_s-\rho_g)g\,\bar{d}_p^3}\right]^{0.029} \left[\frac{\rho_g}{\rho_s}\right]^{0.021} \quad (8)$$

TABLE 3. COMPARISON BETWEEN ACTUAL AND PREDICTED VALUES OF THE COEFFICIENT 'a' IN EQUATION (1)

Material ($\bar{d}_p$ in mm)		$(a)_{exp}$	$(a)_{calc}$ Ergun Eq. (3)	Wen-Yu Eq. (4)	Broadhurst Eq. (5)	Todes Eq. (6)	Sosna Eq. (7)
Corundum	(0.850)	1.338	1.505	1.299	1.433	1.354	1.278
Limestone	(0.565)	1.451	1.584	1.393	1.546	1.464	1.311
	(0.715)	1.296	1.489	1.302	1.457	1.389	1.310
	(0.900)	1.244	1.435	1.250	1.418	1.338	1.296
	(1.125)	1.220	—	—	1.374	1.285	1.284
Lime	(0.565)	1.590	1.607	1.460	1.523	1.518	1.291
	(0.715)	1.414	1.562	1.392	1.495	1.457	1.297
	(0.900)	1.528	1.524	1.346	1.469	1.422	1.281
	(1.125)	1.382	1.490	1.309	1.436	1.377	1.275
Brown	(0.565)	1.403	1.588	1.441	1.519	—	1.294
Coal Ash	(0.715)	1.228	1.538	1.379	1.487	—	1.290
	(0.900)	1.275	1.498	1.333	1.462	—	1.279
	(1.125)	1.195	1.459	1.288	1.428	—	1.271

TABLE 4. COMPARISON BETWEEN ACTUAL AND PREDICTED VALUES OF THE COEFFICIENT 'b' IN EQUATION (1)

Material ($\bar{d}_p$ in mm)		$(b)_{exp}$	$(b)_{calc}$ Ergun Eq. (3)	Wen-Yu Eq. (4)	Broadhurst Eq. (5)	Todes Eq. (6)	Sosna Eq. (7)
Corundum	(0.850)	3.1137	3.5868	3.0055	3.3599	3.1203	2.9088
Limestone	(0.565)	3.0202	3.3763	2.8630	3.2350	2.9682	2.6355
	(0.715)	2.7911	3.3109	2.7802	3.1582	2.9393	2.7879
	(0.900)	2.8371	3.3335	2.7852	3.2189	2.9638	2.8605
	(1.125)	2.8892	—	—	3.2556	2.9709	2.8986
Lime	(0.565)	3.2290	3.3304	2.9774	2.9849	2.9157	2.3933
	(0.715)	2.9434	3.3673	2.9312	3.0793	2.9259	2.5374
	(0.900)	3.4194	3.4447	2.9630	3.1773	3.0020	2.6300
	(1.125)	3.1576	3.4816	2.9600	3.2451	3.0353	2.6783
Brown	(0.565)	2.8645	3.4136	3.0850	3.0560	2.9533	2.3147
Coal Ash	(0.715)	2.5803	3.4416	3.0669	3.1401	2.9767	2.4356
	(0.900)	2.8340	3.5138	3.1019	3.2370	3.0410	2.5085
	(1.125)	2.7395	3.5283	3.0787	3.3029	3.1040	2.6172

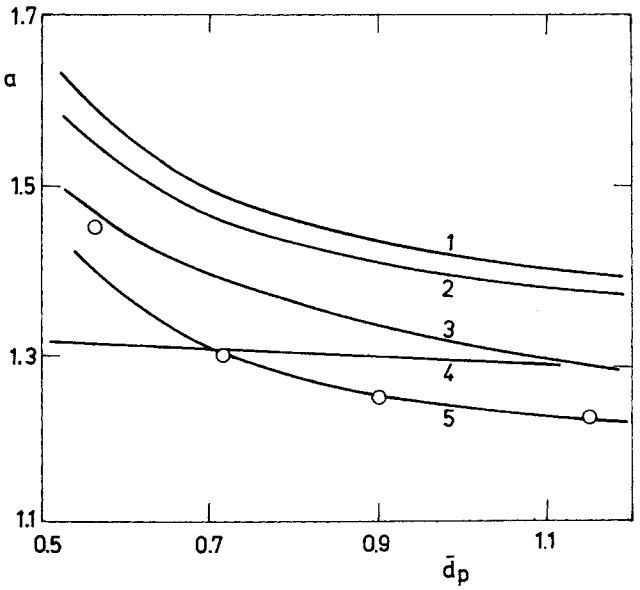

Figure 1. Comparison of the experimental and computed coefficients a in Eq. 1 for limestone: O experimental data points; temperature range, 44-430°C; flow conditions, $1.4 < Re_{mf} < 20$. The solid curves show the values predicted by the individual equations. The physical properties of particles presented in Table 2 were used in computations. Curve 1: Ergun (1952). Curve 2: Broadhurst and Becker (1975). Curve 3: Todes (1957). Curve 4: Sosna and Kondukov (1968). Curve 5: Wen and Yu (1966).

It follows from Eq. 8 that

$$\epsilon_{mf} \doteq \epsilon_{mb} \sim T^{0.0469} \tag{9}$$

which with respect to great sensitivity of G_{mf} to ϵ_{mf} can be significant.

The constants in the Ergun equation can be viewed as modified friction coefficients of a gas moving through the particle bed. They depend on conditions of the whole system and their variation with temperature cannot be ruled out.

The situation is not quite clear with the parameter b. A distinct relationship has not been found by experiments between the values of $(b)_{exp}$ and the particle size nor density. The means values of $(\bar{b})_{exp}$ vary from 2.754 for brown coal ash to 3.187 for lime. Predicted values $(\bar{b})_{calc}$ vary considerably depending upon the equation employed. All coefficients $(\bar{b})_{exp}$ lie in the interval bounded by the values $(\bar{b})_{calc}$ computed from the Ergun and Sosna equations.

NOTATION

a = constant in Eq. 1
b = constant in Eq. 1
$\bar{d}_p$ = mean particle diameter, m
D_K = inside diameter of fluidization reactor, m
g = acceleration due to gravity, $m \cdot s^{-2}$
G = mass velocity of a gas, $kg \cdot m^{-2} \cdot s^{-1}$
H = height of static bed, m

H_K = height of fluidization reactor, m
Δp = pressure drop, Pa
T = absolute temperature, °K
U_f = superficial fluid velocity, m · s^{-1}

Greek Letters

ϵ = bed voidage
ϵ_p = bed voidage obtained by pouring particles
ψ = particle sphericity
μ = viscosity, Pa · s
ν = kinematic viscosity, m^2 · s^{-1}
ρ = density, kg · m^{-3}

Dimensionless Groups

Re_{mf} = $U_{mf}\, d_p/\nu_g$ particle Reynolds number at minimum fluidization velocity
Ga = $\bar{d}_p^3\, \rho_g\, \rho_s\, g/\mu_g^2$ Galilei number

Subscripts

calc = value computed from theoretical equation
exp = value determined experimentally
g = gas property
mb = property at minimum bubbling point of a gas
mf = property at minimum fluidization point
s = property of solid particle

LITERATURE CITED

Broadhurst, T. E., and H. A. Becker, "Onset of Fluidization and Slugging in Beds of Uniform Particles," *AIChE J.*, **21**, 238 (1975).

Desai, A., H. Kikukawa, and A. H. Pulsifer, "The Effect of Temperature Upon Minimum Fluidization Velocity," *Powder Technol.*, **16**, 143 (1977).

Doheim, M. A., and C. N. Collinge, "Effect of Temperature on Incipient Fluidization and Study of Bed Expansion," *Powder Technol.*, **21**, 289 (1978).

Ergun, S., "Fluid Flow Through Packed Column," *Chem. Eng. Prog.*, **48**, 89 (1952).

Saxena, S. C., and G. J. Vogel, "The Measurement of Incipient Fluidization Velocities in a Bed of Coarse Dolomite at Temperature and Pressure," *Trans.*, Instn. Chem. Engr., **55**, 184 (1977).

Sosna, M. C., and N. B. Kondukov, "Criteria and Correlation for Computation of Minimum Fluidization Velocity of Polydispersion Particle Beds," in Russian, *Inzh. Fiz. Zhurnal*, **15**, 73 (1968).

Syromjatnikov, N. I., and V. F. Volkov, "Fluidized Bed," in Russian, Metallurgizdat, Sverdlovsk (1959).

Manuscript received June 9, 1980; revision received October 9, and accepted October 21, 1980.

A Technique for Computer Simulation of Time Varying Slag Flow in a Coal Gasification Reactor

S. R. GOLDMAN

Jaycor, Del Mar, CA 92014

Slag is produced in a slagging coal gasification reactor when devolatilized coal particles burn and leave a residue of molten ash. The ash particles can impinge on the reactor wall and form a film of slag flowing down along the sides of the reactor (Hoy et al., 1965). The flow poses a limit on proper operation in that it can be so great as to plug the tap hole at the bottom of the reactor (Figures 1 and 2).

Although various special cases can be used to estimate the thickness of the slag layer (Bird et al., 1960), computer simulation suggests itself as a means for removing the uncertainty in the estimates as well as for such purposes as determining the heat transport through the slag at all wall locations and the treatment of time varying behavior.

The basic equations determining slag flow are:

$$\frac{\partial \vec{v}}{\partial t} + \vec{v} \cdot \nabla \vec{v} = -\nabla p/\rho + \nabla \cdot (\nu \nabla \vec{v}) + \vec{g} \tag{1}$$

$$\nabla \cdot \vec{v} = 0 \tag{2}$$

$$\frac{\partial y_b}{\partial t} + u_b \frac{\partial y_b}{\partial x} = v_b + S_a \tag{3}$$

$$\frac{\partial T}{\partial t} + \vec{v} \cdot \nabla T = \frac{1}{\rho C_v} \nabla \cdot (k \nabla T). \tag{4}$$

The unknowns are $\vec{v}$, T, p and y_b. For azimuthally symmetric flow, the independent spatial coordinates for the boundary layer are x and y. As one moves along the wall, the x and y axes rotate.

We use the boundary layer approximation (Landau and Lifshitz, 1959):

$$\delta y/\delta x < 1. \tag{5}$$

We note $\rho_1 = Re\ \delta y/\delta x$, whereas $\rho_2 = Re\ Pr\ \delta y/\delta x$.

As an illustration, we consider a reactor with a slag flow rate of 0.1 kg/s, an effective radius at the tap hole of 7.5×10^{-2} m, and ash with characteristics: $k = 1.5$ J/(m · s · °K), $\rho = 2.5 \times 10^3$ kg/m^3, $C_v = 1.8 \times 10^3$ J/kg · °K, $\mu = 1.90 \times 10^8 \exp(-1.07 \times 10^{-2}\, T)$ kg/m · s for $I > I_f$(=1583°K). At T = 1922°K

$$\rho_1 = 0.97\ \delta y/\delta x \tag{6}$$

and

$$\rho_2 = 2.5 \times 10^2\ \delta y/\delta x. \tag{7}$$

From Eqs. 5 and 6, $\rho_1 < 1$; yet simultaneously from Eq. 7, unless $\delta y/\delta x \lesssim 4 \times 10^{-3}$, $\rho_2 > 1$. Hence we set the left hand side of Eq. 1 equal to zero, but we retain the left hand side of Eq. 4. Essentially we are recognizing the condition: $Pr > 1$.

To lowest order in y making use of Eq. 5, we have $h_1 = 1$, $h_2 = 1$, and $h_3 = r - y \cos\theta$. The form for h_3 allows consistently for finite y/r.

For simulational convenience we use variables x', y', and t' so that:

$$\frac{\partial}{\partial t} = \frac{\partial}{\partial t'} - \frac{y'}{y_b} \frac{\partial y_b}{\partial t'} \frac{\partial}{\partial y'} \tag{8}$$

$$\frac{\partial}{\partial x} = \frac{\partial}{\partial x'} - \frac{y'}{y_b} \frac{\partial y_b}{\partial x'} \frac{\partial}{\partial y'} \tag{9}$$

$$\frac{\partial}{\partial y} = \frac{1}{y_b} \frac{\partial}{\partial y'}. \tag{10}$$

On using Eqs. 5 and 8-10, Eqs. 1-4 can be rewritten in conservative form:

$$0 = -\frac{1}{\rho} \frac{\partial p}{\partial x'} + \frac{1}{h_3 y_b^2} \frac{\partial}{\partial y'} \left(\nu h_3 \frac{\partial u}{\partial y'} \right) + g \cos\theta \tag{11}$$

S. R. Goldman is presently with Los Alamos National Laboratory, Los Alamos, NM 87545.

0001-1541-81-4818-0869-$2.00